Surrogate Based Design of a Mooring System for a Self-reacting Point Absorber

Juan P. Ortiz, Helen Bailey, Bradley Buckham, Curran Crawford
West Coast Wave Initiative, University of Victoria,
Victoria, BC, Canada

ABSTRACT

The design of a mooring system for a floating structure is a significant challenge: the choice of line structure and layout determine highly nonlinear hydrodynamic behaviors that, in turn, influence the dynamics of the whole system. The difficulty is particularly acute for floating Wave Energy Converters (WECs) as these machines rely on their movements to extract useful power from wave motions – the mooring must constrain the WEC motion without detracting from power production. To evaluate candidate mooring layouts, a high fidelity representation of the mooring hydrodynamics may be necessary to capture the salient hydrodynamic properties. Unfortunately, high-fidelity modeling tends to be very computationally expensive, and for this reason previous simulation based mooring design largely relies on simplified representations that only reflect part of the mooring design space since some physical and hydrodynamic properties are dropped. In this work, we present how a full hydrodynamic time domain simulation can be utilized within a Metamodel-Based Optimization to better evaluate a wider range of mooring configurations spanning the breadth of the full design space. The method uses a Metamodel, defined in terms of the mooring physical parameters, to cover the majority of the optimization process – the high fidelity model is used to establish the Metamodel in a pre-processing stage. The method was applied to a case study of a two-body heaving point absorber. It was shown that for a two-body self-reacting WEC the mooring loads can have a significant impact on the relative movements of the two bodies and therefore the efficiency of the device. Compared with previous studies on single body WECs, the mooring lines seems to have a bigger impact for self-reacting WEC.

KEY WORDS: Mooring dynamics, Wave Energy Convertor (WEC), Metamodel Based Optimization (MBO).

INTRODUCTION

Mooring system design for a floating structure is a significant challenge as the choice of line structure and layout impacts highly nonlinear hydrodynamic behaviours that, in turn, influence the dynamics of the whole system. Despite advances in mooring line dynamics modeling, conventional mooring system design procedures remain relatively crude. If a mooring is designed to keep a structure stationary and the resulting system displacements are not significant, a simplified static or quasi-static analysis can be used to include the effects of the moorings within investigations of system behaviour. When small displacements cannot be assumed, as for some Wave Energy Converters (WECs), a higher fidelity representation of the mooring hydrodynamics may be required (Fitzgerald & Bergdahl, 2007). High fidelity representations are often completed in the time domain in order to include explicit evaluation of nonlinear loads. But this approach is very computationally expensive. Depending on how the system is represented and the level of detail required, solution of the motion for a particular mooring design iteration and set of wave conditions can range from hours to days. Multiplying that execution time by the number of iterations needed to cover the Design Space (DS) and the range of operating conditions makes strict reliance on high fidelity models infeasible. To date, studies of the impact of the mooring lines on the WEC system dynamics and power conversion have been completed by applying simplified models and/or sensitivity studies that indeed cover part of the DS, but do not include all the possible mooring configurations.

One such approach is presented by (Fitzgerald & Bergdahl, 2007). The mooring lines effects are included into the frequency domain by calculating an equivalent linear impedance from a non-linear model, run in the time domain. In that work, four different mooring lines configurations were evaluated for a simplified WEC that extracts power for surge, heave and pitch motions. The linear model applied has favourable run times, but neglects nonlinear effects created by line drag and large changes in the mooring geometry. Fitzgerald & Bergdahl concluded that the mooring loads can have an important effect on the WEC movement and therefore on the energy harvesting (Muliawan, et al., 2013) presented a sensitivity study based on 6 different mooring systems configurations; the study was carried in the time domain using a commercial software that considers the hydrodynamics, Power Take

off (PTO) and mooring loads. The mooring loads were simulated as a nonlinear spring with no drag or inertia loads calculated over the mooring lines. Muliawan, et al. (2013). concluded that even though the tension loads were not completely accurate, the impact of the mooring lines on the device in regular waves can vary the total power adsorption between +4% to -8%, when compared to the case with no moorings. With irregular waves, the impact is smaller, around 1.1%. Another study was presented by Cerveira et al. (2013) who considered an arbitrary floating WEC in both the time and the frequency domain. To facilitate the frequency domain analysis, the mooring lines were included into the model as forces proportional to the displacements and the velocity, and the PTO extracted power from the heaving and surging motion of a single buoy. Two mooring configuration were considered and compared to the unmoored system; it was found that the influence of the mooring on power production was small. In individual sea states the idealized WEC show a decrease in the power capture between 0.5% and 1.5% for a slack mooring configuration and around 1% on the total annual energy capture. The author comments that results are valid for the hypothetical WEC and further investigation is require for a more realistic device.

Use of formal optimization in WEC mooring design was executed by Vicente, et al. (2011) for a single hemispherical floating WEC subject to regular waves; two mooring lines configurations were considered and the power was extracted by a linear PTO that is proportional to the absolute heave displacement. Vicente et al.'s study focussed on the influence of the mooring system parameters on the power absorption and the horizontal displacement. It revealed that the single body WEC considered was influenced by the mooring lines - power conversion could be changed in some extent through the selection of the mooring parameters. Investigation is needed into two-body self-reacting WECs mooring lines configurations, as there is a great opportunity to influence power conversion, since these devices rely on relative motion of the two-bodies.

In this work, a comprehensive treatment of the mooring line dynamics is included in a mooring line optimization study for a two-body, self-reacting, heaving WEC. Power conversion performance in operational conditions is used as the sole metric for evaluating the various mooring candidates – survivability concerns are not included at this time. A fully non-linear time domain simulator is used to capture the coupled mooring, WEC and PTO dynamics. The moorings are represented as a cubic-spline lumped mass cable model that includes drag, weight, floor friction, torsional and bending stiffness (Buckham, 2003). The proposed WEC consists of a conventional co-aligned axisymmetric point absorber; the WEC hydrodynamic model considers radiation and diffraction effects, as well as non-linear drag over the WEC's component hulls. The environmental conditions used to evaluate the system performance are drawn from a resource assessment currently being completed for the Pacific coast of Canada, by the West Coast Wave Initiative, located at the University of Victoria. In order to mitigate the longer run times required by the non-linear dynamics simulator, the WEC mooring DS is explored by using a MBO routine. The MBO technique uses data calculated a priori using the full simulator to form a Meta-Model (MM) that emulates the high fidelity simulators estimation of performance at any point in the DS.

The paper is structured as follows: The features of the case study two-body WEC are presented in Section 2. Section 3 outlines the mooring design variables. In Section 4 the optimization algorithm used to traverse the design space is described. The results, including identified locally optimal configurations and the mooring impacts on performance are discussed on Section 5 and, Section 6 summarizes the main findings and future work.

WEC DYNAMICS MODEL

An axisymmetric point absorber formed from two coaxial bodies, a toroidal float and a central spar, connected by a coulombic PTO was considered. The PTO produces a force proportional to the relative velocity and the constant of proportionality is adjusted to match the real part of the radiation impedance of the system, in order to absorb the largest amount of energy (Falnes, 1998). The WEC corresponds to a full-scale version of the scale model described by Beatty et al. (2014). Further information about the full scale model is provided by Bailey et al. (2014).

Parameter	Units	Value
Spar Mass	Kg	1646875
Spar Moments of inertia (Ixx_{Cg_S}, Iyy_{Cg_S}, Izz_{Cg_S})	Kgm^2	5656250, 5656250,648437.5
Float Mass	Kg	201406.25
Float Moments of inertia (Ixx_{Cg_f}, Iyy_{Cg_f}, Izz_{Cg_f})	Kgm^2	5785156.25,5785156.25, 1445312

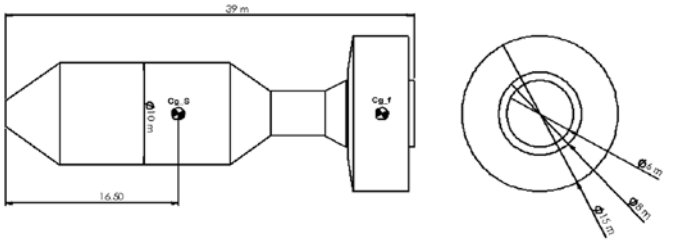

Fig. 1 The two-body heaving point absorber considered in the mooring design study.

Hydrodynamic Loads

The study case was implemented within the software package ProteusDS; a finite element, non-linear, time domain solver used for dynamic analysis of WEC and wave interactions. The software capabilities includes non-linear cable dynamics, interconnections of articulate hulls and mooring lines, PTO dynamics, viscous drag forces and wave radiation and diffraction loading (Steinke et al. 2008, Nicoll, et al. 2012) .

The Froude-Krylov and buoyancy forces that act over the spar and float were calculated by integrating the undisturbed pressures over the wetted area of the WEC. For this calculation, the spar and float surfaces were discretized into panels and the wetted area was calculated based on the current position and orientation of each body. This results in a nonlinear force, since it accounts for significant changes in wetted area created by large displacements of the two bodies.

The other component of the excitation force, the scattering force, is obtained from WAMIT (a commercial software which uses flow potential theory and boundary element method to obtain hydrodynamic parameters). The radiation force is obtained from the convolution of the impulse response kernel obtained from the frequency dependent damping terms, the velocity time history of the bodies and the added mass at infinity frequency. The coupled radiation and excitation forces (due to one body interacting with the other) are not included. The nonlinear viscous drag effects where included into the model according to Morrison's equation. The drag coefficient in heave was obtained from experimental data presented by Beatty et al. (2014) and the surge and sway drag coefficients were used according to Babarit, et al. (2011).The drift effects due to the second order wave forces are not included in these simulations. The drift effects are caused by the total pressure difference between the forward and aft surfaces of the bodies

due to its asymmetric wetted surface.

The mooring line dynamics were incorporated into the simulation using a finite-element method that is based on a cubic-spline element geometry. The cable model employs a lumped mass approximation to the cable continuum and calculates the drag, added mass, weight and seabed friction forces at the node points. Cable node accelerations are calculated explicitly and the cable state is evolved with the WEC position and orientation using an adaptive Runge-Kutta integration scheme. The cable element tensions, including at the boundary node at the fairlead location on the spar, are recovered from the current values of the cable node positions using constitutive relations. For the details of the cable model, the reader is referred to (Buckham, et al., 2004) (DSA, 2013).

Environmental Conditions

The sea state used for the optimization was carefully selected in other to embrace the specific qualities of the WEC. A 2.75 m wave height and a 9.5 seconds energy period of were selected, as this sea state is close to the natural frequency of the device and also corresponds to the most energetic sea at Amphitrite bank, a high wave energy location (Robertson et al. 2014). For this particular study, a depth of 40m was considered with no variations due to tides. The current and wind loads were ignored and a JONSWAP wave spectrum was considered to represent the sea state.

OPTIMIZATION PARAMETERS

Any single mooring configuration must be completely described by the design variables used in the optimization; these include line material, diameter, number of mooring lines, size and location of subsurface floats etc. For this analysis, six design variables were chosen. These were selected by comparing what has been done by different authors on previous works, (Muliawan et al., 2013)(Cerveira et al., 2013)(Vicente et al., 2011) and are believed to yield a broad design space that extends beyond conventional mooring configurations – they provide opportunity to uncover innovative mooring configurations. Table 1 summarizes the 6 design variables:

Table 1.Optimization parameters

Parameter	Minimum	Maximum
Number of Lines	3	4
Float Diameter (Percentage of total line weight)	0	100%
Line Slope	1:4	4:1
Connection Point on the *Spar*	11.19 m	25 m
Line diameter	0.02 m	0.12 m
Float location (distance along line from spar to anchor)	10%	30%

The first parameter considered was the number of lines: only values of 3 and 4 lines were allowed, as existing literature shows these arrangements to be necessary to moor a device in storm conditions (which are otherwise not considered in this work) (Muliawan et al., 2013)(Cruz et al, 2013). The lines were always arranged axisymmetrically: 120 degree separation when the mooring system had 3 lines and 90 degree separation when 4 were used.

Chain grade R4 was considered according to (DNV, 2010) and only the chain diameter was adjusted. The slope of the lines was defined as shown in Fig. 2. When the slope is long and the uplifting forces are near zero, drag anchors are considered; for steeper slopes, plate anchors are used. An extra 30% of line was considered, to maintain slack in the line. The maximum line floats volume is defined by the weight of a line with a length equivalent to the distance between the connection point in the spar and the anchor connection; for this calculation, the slack in the line was not considered in order to have the line sitting at the seabed as the initial condition. As the main interest of this paper is to study how the mooring lines affect the power extraction; the pretension of the line was controlled indirectly by considering different combinations of chain diameter, slope and connection height. A sample simulation for a single design variable set is presented in Fig. 2.

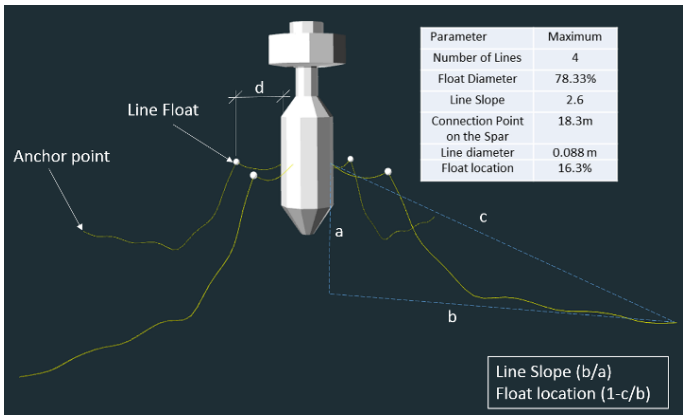

Fig. 2: Mooring configuration example.

NUMERICAL OPTIMIZATION

The objective function (OF) for the optimization routine is defined by the average power in operating conditions for the WEC. To evaluate the OF, a nonlinear high fidelity time domain representation of the system is required. This simulation is very computationally expensive, which makes reliance solely on this kind of models infeasible. In order to mitigate the longer run times required by the non-linear dynamics simulator, the WEC mooring DS is explored by using a MBO routine; whereas the high fidelity simulation is embedded inside the optimization process.

A MBO is a technique devised to study the DS associated with computationally-expensive OF where a Meta-Model (MM) is constructed using specific points evaluated on the high fidelity simulators which are then fitted in a hypersurface. The MM can be used as the OF to optimize the system with a lower computational cost, as the high fidelity model only needs to be evaluated a limited number of times (Cavazzuti, 2013).

As shown in Fig. 3, the first step of the process consists of gaining knowledge of the OF's shape across the DS by evaluating the OF over a sparse set of sampling points. The first sampling points are selected applying a Design of Experiment (DOE) strategy; then, using the collected information, a MM is constructed that can then be used to estimate the OF at any point in the DS. Using the MM the next points to evaluate are selected considering their possible impact on the model. The idea is to pick the points with the highest information contribution to the MM, so they can be used to validate the model and improve its accuracy by incorporating them into the data pool and recalculating the MM coefficients. Finally, the observations are used to explore the DS and find the minimum of the OF. If the found point meets the

termination criteria, the optimization is terminated. If it does not, the process is repeated, until the criterion is met (Forrester, Sóbester, & Keane, 2008). The MBO was implemented using the Matlab toolbox MATSuMoTo (Muller, 2014).

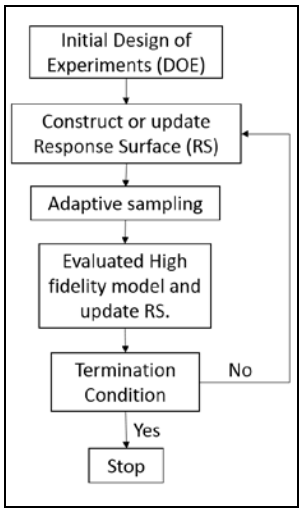

Fig. 3: Optimization process

Design of Experiments

At the beginning of the process, a DOE is used to strategically select sample points in the DS. Several techniques have been developed for executing a DOE. These include Factorial Full, Factorial Central Composite, Latin Hypercube, etc. (Cavazzuti, 2013). In this work, a Latin Hypercube is used. This method generates samples over the DS by dividing it into subspaces and then selecting plausible configurations on the multidimensional DS, in such a way that each sample point is the only one in each aligned hyper plane (Cavazzuti, 2013). Thirty points in the 6 dimensional DS were used for the DOE – these spanned the intervals defined in Table 1. Figure 4 shows the sampled points over the DS.

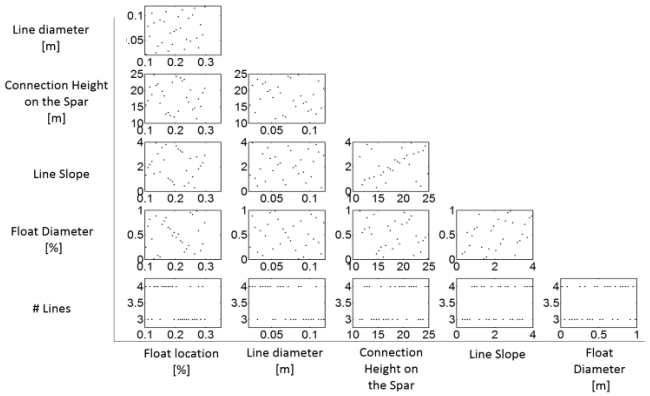

Fig. 4 : Selected DOE points. Each window represents a planar projection of the hyperdimensional design space. As only two values are possible for the parameter "# Lines", it is represented by two lines. The other parameters are considered continuous over the DS; therefore their distribution is broader.

Meta Model

Results gathered by the DOE, are used to create a response surface or MM. A MM consists of a mathematical representation of a more complex system, where coefficients are fit in order to approximate the DS. Even though this model will not yield to the exact solution of the problem, it can be used to efficiently estimate the optimum design point. This makes it a powerful tool when the OF must be calculated with a computationally expensive simulation. For this technique to work, the MM form needs to be selected carefully in order to accurately describe the DS. The large number of mathematical models that exist make this selection a challenging decision, as normally little information about the system is known before starting the optimization process. In this paper a weighted combination approach is used, according to Mueller & Piche (2011). The basic idea consists of using different MMs that are added together using a weighted sum model. The predicted model $\hat{f}(x)$ of the mixed MM can be generalized as

$$\hat{f}(x) = \sum_{i=1}^{N} w_i \hat{f}_i(x)$$
$$\sum_{i=1}^{N} w_i = 1 \quad (1)$$

Where x is a vector that contains the design parameters $\hat{f}_i(x)$ represents the predicted value of each model, w_i the corresponding weight and N the number of models. The weights are calculated according to Dempster-Shafer theory, which allows to combine information from different sources, even when it seems contradictory, in order to build a degree of belief. The idea consist on combining the MMs according on how good they describe the real DS, represented by the sample points. Each MM is evaluated according to its correlation coefficients, root mean square errors and median absolute deviation. A good DS representation has a high correlation coefficient and low root mean squared errors and median absolute deviation. Sometimes these coefficients can present contradictory information; Dempster-Shafer theory can be applied to find the probability for each representation and to assign a weight to each MM.

In this paper, a combination between a Kriging model and Multivariate Adaptive Regression Splines (MARS) is considered. Kriging is a regression Gaussian process which uses a weighted average of known values to predict a point in the same neighborhood. Mathematically, it is defined as:

$$\hat{f}(x) = f(x) + Z(x) \quad (2)$$

Where f(x) represents the global model and Z(x) the local deviation, defined as a stochastic process realization with mean zero and non-zero covariance. As the DS is globally approximated by f(x), Z(x) adds local deviations, in order to interpolate the sample points using a define function to predict the correlation function for the stochastic processes. For this paper, first order polynomials has been used to approximate the global space, and a spherical correlation function to interpolate the local deviations. This model was implemented using Matlab toolbox DACE (Lophaven, et al. 2002).

The MARS algorithm considers a non-parametric weight sum regression technique (Gints & ARESLab, 2011):

$$\hat{f}(x) = \sum c_i B_i(x)$$
$$\hat{f}(x) = c_1 \max(0, x - a_1) + c_2 \max(0, x - a_2) \ldots \quad (3)$$
$$+ c_3 \max(0, x - a_3) \max(0, x - a_4) + \ldots$$

where c_i are constant coefficients related to the best fit of the data, Bi(x) are the basic functions defined by combinations of the hinge equation, and a_i (referred to as "Knot") are constants in the hinge equation. As part of the range of a hinge function is zero, it can be used to partition the data into disjointed regions, which can be treated independently.

Then, the MM is built by a two phase iterative approach. The first step consists of building a model using a forward strategy, in which a new equation is added after each iteration, beginning with the intercept and then continuing with a pair of equations based on the hinge function. In each step, the required coefficients are fitted, by reducing the mean square error of the residuals. The process stops when the residual error is too small or when the number of iterations, defined by the user, is reached. In the second part of the process, terms are removed from the model, one by one, until the best representation is found. The performance of the different subsets of the model are compared using a cross validation scheme, where at least one of the training points is not included on the fitting process, so it can be used to calculate the error of the model.

Adaptive Sampling

In order to keep the evaluations of the high fidelity model to a minimum, it is important to define a strategy to select the candidate points that contribute the most information and lead to a converged solution as quickly as possible. The strategy selection will be linked to the end purposes of the model: if only a local exploration is required, the new samples should be selected so as to improve the accuracy in the neighborhood of the optimum points predicted by the MM. On the other hand, if a complete DS exploration is required, the infill strategy should be such that general accuracy is enhanced by selecting the samples on the less explored areas (Muller et al., 2013). A third strategy is to combine both approaches by increasing the resolution of the model near feasible points, but also exploring less populated areas that could lead to a better solution.

For this work, the algorithm considered is based on this idea (Muller, Shoemaker, & Piche, 2013). It contemplates 4 different regions where candidate samples are picked. The first group of candidates is generated by keeping the discrete variables near the most feasible point constant and perturbing the continuous variables, by randomly adding and subtracting small, medium and large perturbations. The second group is prepared in the opposite way: the discrete variables are perturbed and the continuous variables are kept constant. The third group is generated by perturbing both the discrete and the continuous variables near the most feasible point, by randomly adding and subtracting small, medium and large perturbations. The last group is constructed by randomly sampling the DS in order to ensure that every point has a positive probability of being picked. After all the sample points are generated, the best candidates are determined using two scoring criteria. The first criterion calculates the score using the OF value predicted by the MM; the difference between the predicted minimum and the possible sample is calculated and normalized by the difference between the predicted maximum and minimum points.

$$V_R = \frac{\hat{f}(x_i) - \hat{f}(x_i)_{\min}}{\hat{f}(x_i)_{\max} - \hat{f}(x_i)_{\max}} \tag{4}$$

The second criterion is derived from the distance between the candidate point and the already sampled points. For each candidate, the Euclidean distance to the already evaluated points are calculated and the maximum and minimum distance for all the possible candidates are defined. Then the score is defined by the difference between the minimum distance calculated of a particular candidate and the maximum distance calculated for all possible candidates and normalized by the difference between the maximum and minimum differences for all possible candidates.

$$V_D(x_i) = \frac{\Delta_{\max} - \Delta_{\min}(x_i)}{\Delta_{\max} - \Delta_{\min}} \tag{5}$$

where $\Delta_{\max}$ and $\Delta_{\min}$ are the maximum and minimum distances for all possible candidates and $\Delta_{\min}(x_i)$ is the minimum distance for a particular candidate.

Finally, a weighted sum is used to determine the final score for each candidate. In order to prevent instabilities in the model, the weights are adjusted in a cyclical manner, beginning with high weight for the distance score and low score for the prediction score. In this way, the search at the beginning is more global than local. As the optimization process continues this relation changes in order to focus more on the located minimum. Then when a cycle has ended the roles are inverted for the process to begin again.

For this study eight samples were incorporated in every step of the infill

Termination Condition

As explained by Muller, Shoemaker, & Piche (2013) the algorithm considerate is asymptotically complete, which means that if it is run long enough, it will converge to a global minimum; for practical reasons, the termination condition was defined by maximum number of allowed iterations. For a time frame of 15 days to solve the optimization problem, and a period of approximately 15 hours per simulation, and 8 models run at the same time, 200 iterations were selected.

RESULTS AND DISCUSSION

A unimodal optimization scheme was implemented in order to conduct a preliminary study of the influence of the mooring lines on the total power recovered. For this study, cost, survivability, sea keeping, stresses and avoidance of snap loading on the mooring lines have not be considered but will be implemented in future work. The OF was based on the average power extracted over a 300 seconds time domain simulation, ignoring the initial 100 seconds of the transient start-up. The most energetic sea state over a year, at Amphitrite Bank in BC, Canada was considered for this study. After 200 iterations, an optimum mooring configuration was found that improves the power extraction of the WEC in the defined conditions. Figure 5 presents the contour plot of the MM in the same neighborhood as the found optimum configuration. For each window, four of the six parameters were kept constant and equal to the optimum

.

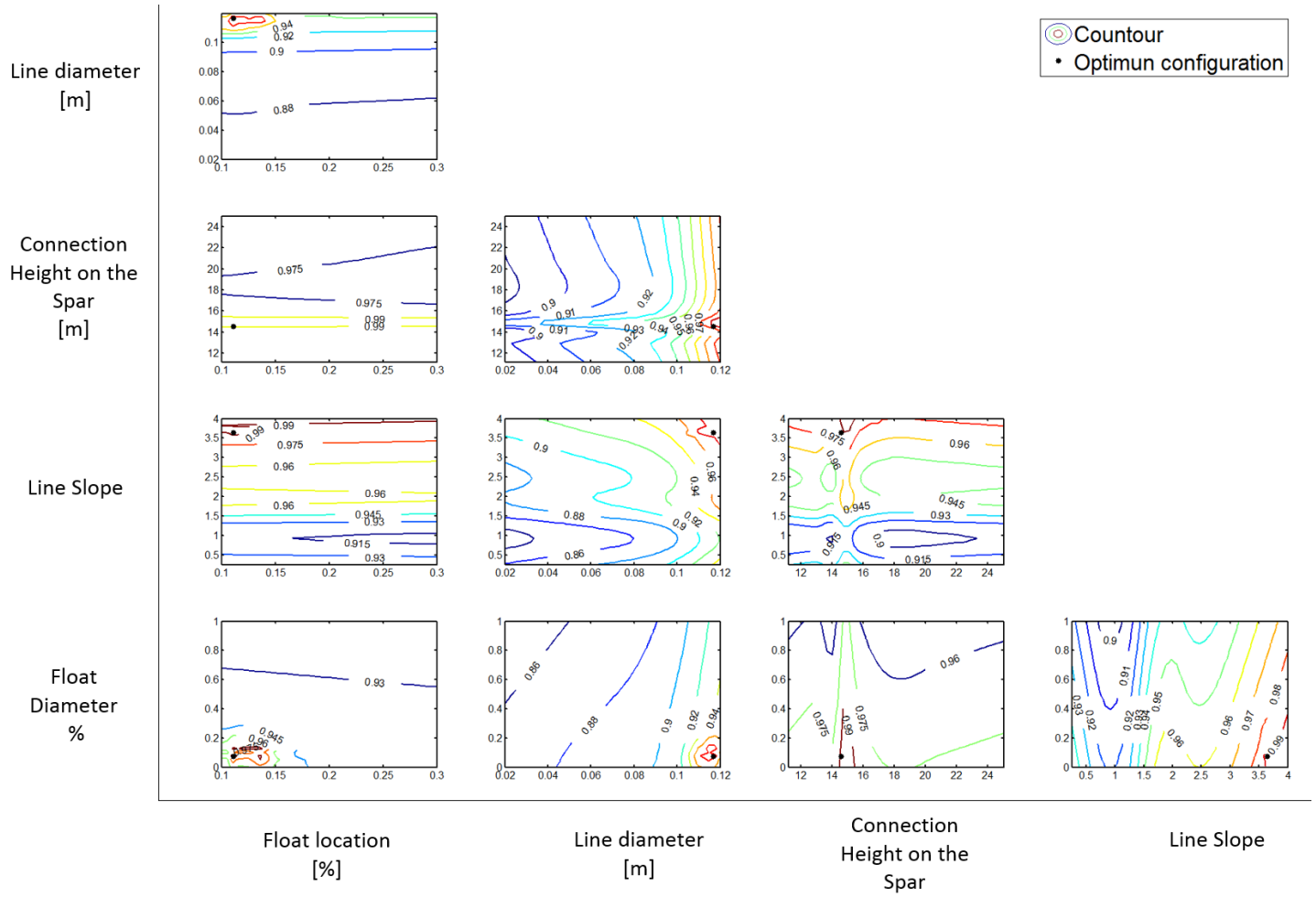

Fig. 5: Contour plots: The contour plot shows in each window the normalized maximum instantaneous power vs two of the optimization parameters. The power is normalized by the maximum power found. Each window plot is built by keeping four of the six parameters constant and equal to the optimum value, while the other two parameters were varied through the entire DS. The 4 leg configuration is kept constant throughout the contour, as only 2 options were include into the optimization routine.

value as the other two parameters were varied through the entire DS for the 4 lines configuration. From the contour plot it can be observed that the device has a better performance when the moorings are connected near the center of the rotation of the WEC and this WEC is particular sensitive to this parameter as small changes in the connection height have a large influence on the power recovered. This could be as at this connection height, the moorings are not inducing moments into the system that can adversely affect the performance of the device

By studying the contours it can be appreciated that for this particular sea state the WEC has better performance with four lines, larger line slope and line diameter. It seems that when the mooring lines are longer and thicker, they have a greater resistance to motion, as the spar of the WEC is directly influenced by the mooring lines this changes the behaviour of the system. This can be seen in Fig. 6, where the instantaneous relative position, velocity, and PTO force are shown for part of the time series.

A slack moored mooring system incorporates a resistive and restorative force to the system. As the WEC is drawn away from its initial position by the sea, the mooring lines are raised from the floor, instantaneously adding new loads to the system, which change how the device is behaving. This change in the system behavior seems to make the difference between the moored and unmoored configuration. In Fig. 7 the same time slot is shown for the instantaneous power.

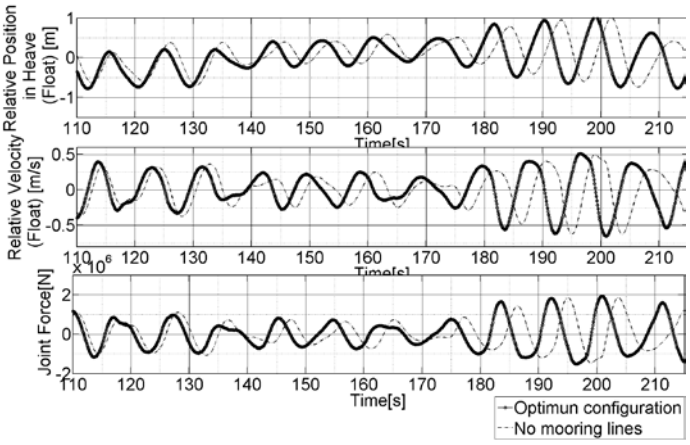

Fig. 6 Relative displacement, velocity and joint force.

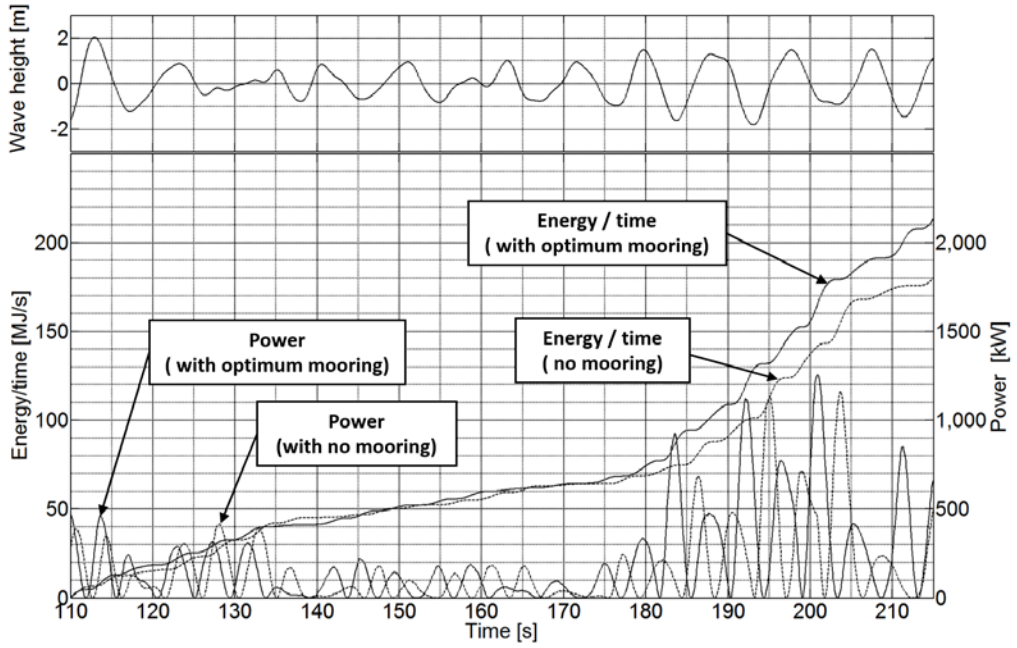

Fig. 7: Power [kW], Energy /Time[MJ/s], Wave Height [m]

By comparing both figures, it seems that the selected configuration changes the way that the *spar* behaves, shifting its movements and increasing the relative displacement between the two bodies, therefore increasing the energy extracted in the time period. In Fig. 8 the RAO of the relative displacement of the two bodies is presented.

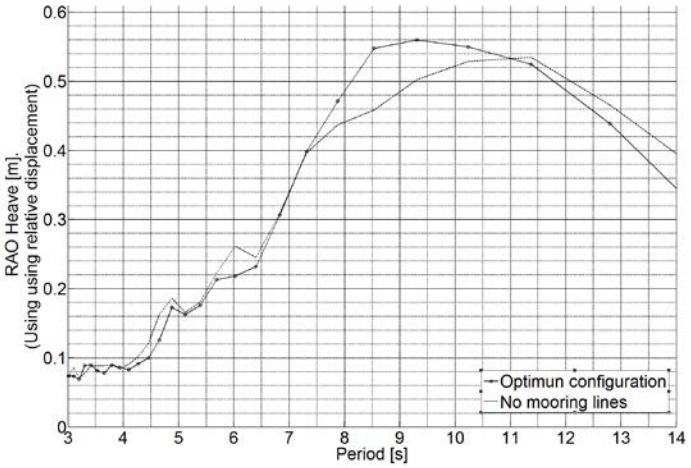

Fig. 8: RAO Heave (Were obtained using a FFT over the relative displacement of the WEC. For smoothing the response the data was divided and overlapped using a hamming window.)

The moorings lines are changing the system phase and natural frequency improving the total performance and the overall energy extraction.

After studying the whole time series, it has been determined that the *spar* mainly reacts with the mooring line and only occasionally the mooring line becomes taut and apply a force directly to the anchors. Furthermore, it was observed that the maximum instantaneous power occurred when the moorings were taut. Another noteworthy that when the waves period are between 7.5s and 11s, the WEC behaves better

without reacting with the anchors and the energy extracted grows faster for the optimum configuration as shown in Fig. 7 between 110s and 215s

The snap loads on the anchors and the moorings due to the mooring lines going taut is an important issue that can only be fully studied by including survivability constrains on the model, which has not been yet implemented. In order to get an idea of the magnitude of the stresses on the lines, the tension loads for the optimized case were plotted in Fig. 9.

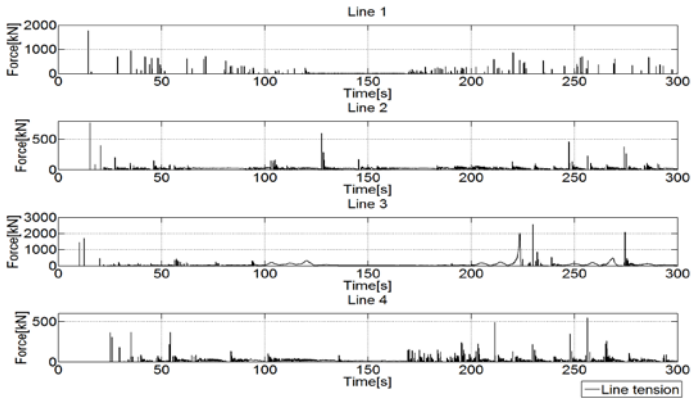

Fig. 9 Mooring lines loads

The predicted breaking strength for a R4 chain of 120 mm is 13,000 kN according to Johanning, Wolfram, & Smith (2006). Fig. 9 shows that the typical load at the considered case is low, even for the third mooring line which is aligned with the wave incident direction. When the line snap higher tension loads are observed, these are still below the allowable strength. For the maximum tension load at 230 seconds, a safety factor of 5 was obtained.

It can be seen that the optimum configuration extracts around 24% more power at the defined conditions when it is compared to the unmoored configuration.

Table 2 Result summary table

		Optimum values	Optimum configuration eliminating line floats
Parameters	Number of Lines	4	4
	Float Diameter (%)	7.3	-
	Line Slope	3.6	3.6
	Connection Point on the *Spar* (m)	14.6	14.6
	Line diameter (m)	0.12	0.12
	Float location (%)	12	12
	Average power (kW)	27.7	25.9

CONCLUSIONS

It has been shown that an MBO routine can be used to optimize a mooring line configuration for a WEC using a high fidelity model. This approach allows us to assess the whole mooring DS to obtain a better understanding of the system behavior.

After 200 evaluations of the high fidelity model a pseudo-optimal configuration was obtained which improved the power extraction of the WEC considered. This proved the importance of assessing the whole mooring DS. It has also been shown that for this particular WEC that the non-linear loads of the mooring lines play an important role on the machine tuning, as they highly impact the response of the device and therefore its efficiency. Further investigation is required as the optimization routine that was run only includes average power in the OF for a single sea state. Constraints must be added to the formulation, including cost, survivability, seakeeping, stresses and avoidance of large snap loading on the mooring lines. The problem could be reformulated to include this parameters in a multi-OF. Also, as some of the optimum parameters are on the limit of the DS (line diameter, slope), it is required to expand the allowable range.

ACKNOWLEDGMENT

This work was funded by Natural Resources Canada, the Pacific Institute of Climate Solutions and the Natural Sciences and Research Council of Canada. The first author also wants to acknowledges the additional funding from Minister of Science Technology and Telecommunications of Costa Rica (CONICIT) .

REFERENCES

Babarit, A., Hals, J., Kurniawan, A., Muliawan, M., Moan, T., & Krokstad, J. (2011). *Numerical estimation of energy delivery from a selection of wave energy converters.* Norway.

Bailey, H., Ortiz, J. P., Robertson, B., Buckham, B. J., & Nicoll, R. S. (2014). A Methodology for Wave-to-Wire WEC Simulations. *2nd Marine Energy Technology Symposium* (p. 15). Seattle, WA: METS2014.

Beatty, S., Hall, M., Buckham, B. J., Wild, P., & Bocking, B. (2014). *Experimental and numerical comparisons of self-reacting point absorber wave energy converters in regular waves.*

Buckham, B. J. (2003). Dynamics modelling of low-tension tethers for submerged remotely operated vehicles. *University of Victoria*.

Buckham, B., Driscoll, F., & Nahon, M. (2004). Development of a Finite Element Cable Model for Use in Low-Tension Dynamics Simulation. *Applied Mechanics*, 476-485.

Cavazzuti, M. (2013). *Optimization Method: From Theory to Design.* New York: Springer Heidelberg.

Cerveira, F., Fonseca, N., & Pascoal, R. (2013). Mooring system influence on the efficiency of wave energy converters. *International Journal of Marine Energy*, 65-81.

Cruz, J., Mackay, E., Livingstone, M., & Child, B. (2013). Validation of Desigm and planning tools for wave energy converters. *1st Marine Energy Technology Symposium* (p. 12). Washinton D.C USA: METS13.

DNV. (2010). *DNV-OS-E301*. Norway: Det Norske Verits.

DSA. (2013). *ProteusDS 2013 Manual.* Victoria, BC, Canada.

Falnes, J. (1998). Wave Energy Conversion Through Relative Motion Between Two Sigle Mode Oscillation Bodies. *Offshore Mechanics and Arctic Engineering*, 32-38.

Faltinsen, O. M. (1990). *Sea Loads on Ships and Offshore Structure.* Cambridge,United Kingdom: Cambridge University Press.

Fitzgerald, J., & Bergdahl, L. (2007). Including moorings in the assessment of generic offshore wave energy convertor: A frequency domain approach. *Marine Structures*, 23-46.

Forrester, A., Sóbester, A., & Keane, A. (2008). *Engineering Design via Surrogate Modelling.* Southampton: John Wiley and Sons, Ltd.

Gints , J., & ARESLab. (2011). *Gints Jekabsons*. Retrieved from Adaptive Regression Splines toolbox for Matlab/Octave: http://www.cs.rtu.lv/jekabsons/

Johanning, L., Wolfram, H.-J., & Smith, G. H. (2006). Mooring desing approuch for wave energy converters. *Journal of Engineering for the Maritime Environment*, 159-174.

Lophaven, S., Nielsen, H. B., & Søndergaard, J. (2002). *DACE:A MATLAB Kriging Toolbox.* Lyngby – Denmark, Lyngby, Denmark.

Muliawan, M. J., Gao, , Z., Moan, T., & Babarit, A. (2013). Analysis of Two Body Floating Wave Energy Converter with particular focus on the effects of the power take off and mooring systems on energy capture. *Offshore Mechanics and Artic Engineering*.

Muller, J. (2014). *MATSuMoTo*. New York: Cornell University.

Muller, J., & Piche, R. (2011). Mixture Surrogate Models Based on Dempster-Shafer Theory for Global Optimization Problems. *Journal of Global Optimization*,, 51-79.

Muller, J., Shoemaker, C., & Piche, R. (2013). *SO-MI: A surrogate model algorithm for computationally expensive nonlinear mixed-integerblack-box global optimization problems.* UnitedStates: Computers & Operations Research.

Nicoll, R., Wood, C., & Roy, A. (2012). COMPARISON OF PHYSICAL MODEL TESTS WITH A TIME DOMAIN SIMULATION. *International Conference on Ocean, Offshore and Arctic Engineering* (p. 10). Rio de Janeiro, Brazil: ASME.

Robertson, B., Hiles, C., & Buckham, B. (2014). Characterizing the near shore wave energy resource on the west coast of Vancouver Island, Canada. *Renewable energy*, 665-678.

Steinke, D. M., Nicoll, R. S., & Buckham, B. J. (2008). Design Through Simulation: Finite Element Capabilities for Ocean Engineering. *Ocean, Offshore and Arctic Engineering Division* (pp. 339-348). Estonil, Portugal: ASME.

Vicente, P., Falcao, A., & Justino, P. (2011). Optimization of moorings configuration parameters of floating wave energy converters. *ASME 2011 30th International Conference on Ocean, Offshore and Artic Engineering* (p. 7). Netherlands: ASME.